Tetrahedron Lett. Author manuscript; available in PMC 2020 February 21.

Published in final edited form as:
Tetrahedron Lett. 2019 February 21; 60(8): 594–597. doi:10.1016/j.tetlet.2019.01.029.

Mycopyranone: a 8,8'-binaphthopyranone with potent anti-MRSA activity from the fungus *Phialemoniopsis* sp

José Rivera-Chávez[a,c], **Lindsay Caesar**[a], **Juan J. Garcia-Salazar**[a], **Huzefa A. Raja**[a], **Nadja B. Cech**[a], **Cedric J. Pearce**[b], **Nicholas H. Oberlies**[a]

[a]Department of Chemistry and Biochemistry, University of North Carolina at Greensboro, Greensboro, North Carolina 27412, USA.

[b]Mycosynthetix, Inc., Hillsborough, North Carolina, 27278, USA.

Abstract

A new 8,8'-binaphthopyranone (mycopyranone, **1**) was isolated from a solid fermentation of *Phialemoniopsis* sp. (fungal strain MSX61662), and the structure was elucidated via analysis of the NMR and HRESIMS data. The axial chirality of **1** was determined to be *M* by ECD. The central chirality at C-4/C-4' was assigned through a modified Mosher's method, while the absolute configuration at C-3/C-3' was deduced based on analysis of the $^{3}J_{H\text{-}3\text{-}H\text{-}4}$ values and NOESY correlations. Compound **1** was evaluated for its antimicrobial properties against *Staphylococcus aureus* SA1199 and a clinically relevant methicillin-resistant *S. aureus* strain (MRSA USA300 LAC strain AH1263). Compound **1** inhibited the growth of both strains in a concentration dependent manner with IC_{50} values in the low μM range. Molecular docking indicated that compound **1** binds to the FtsZ (tubulin-like) protein in the same pocket as viriditoxin (**2**), suggesting that **1** targets bacterial cell division.

Graphical Abstract

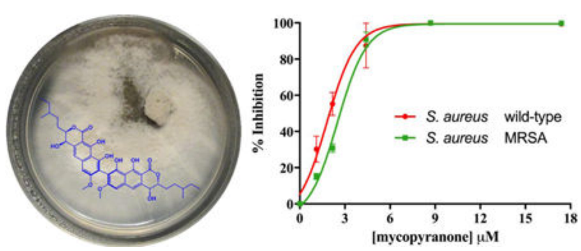

[c]Current address: Department of Natural Products, Instituto de Química, Universidad Nacional Autónoma de México, Ciudad de México 04510, Mexico

Supplementary data

Supplementary data (Phylogenetic analysis of *Phialemoniopsis* sp., 1D and 2D NMR data of compound **1**, HRESIMS of compound **1**, concentration response curve of berberine, and structural model of compound **1**-FtsZ) associated with this article can be found, in the online version.

INTRODUCTION

Nosocomial infections caused by methicillin-resistant *Staphylococcus aureus* (MRSA) are a serious health problem.[1–3] In the United States alone, over 80,000 severe MRSA infections were documented in 2013, 11,000 of which were fatal.[4] Unfortunately, despite the imminent problem MRSA and similar drug resistant infections pose, most pharmaceutical companies do not focus on the discovery and development of new antimicrobial agents.[5, 6] In this context, the World Health Organization has started a cooperative program with Academia to search for new molecules and strategies to combat antibiotic resistance.[7, 8]

One promising strategy to combat MRSA infections is targeting cell division via the inhibition of the proto ring protein FtsZ,[2, 9] a vital and highly conserved protein involved in bacterial division and formation of new cells; it is a homolog of tubulin in eukaryotic cells.[10, 11] However, despite the importance of this protein as a molecular target to combat infections against MRSA, just a few examples of molecules have been described as potential inhibitors, including natural products[12–16] and synthetic probes.[9, 17] Among natural products, viriditoxin (**2**), a 6,6'-binaphthopyranone, inhibited the polymerization of FtsZ, resulting in the inhibition of bacterial cell division, and this compound has been proposed as a promising lead for the development of anti-MRSA drugs.[16, 18]

As part of ongoing studies to identify structurally diverse and bioactive metabolites from fungal cultures, a new 8,8'-binaphthopyranone derivative (mycopyranone, **1**) was isolated from *Phialemoniopsis* sp. (strain MSX61662), which was identified phylogenetically and morphologically using methods that were detailed previously.[19, 20] The structure of **1** was established using a set of spectroscopic (1D and 2D NMR), spectrometric (HRESIMS), and chiroptic (ECD and OR) methods. The antimicrobial activity of **1** was evaluated against *Staphylococcus aureus* SA1199[21] and a clinically relevant methicillin-resistant *S. aureus* strain (MRSA USA300 LAC strain AH1263).[22] Growth inhibition by **1** was noted in both strains in a concentration dependent manner with IC_{50} values in the low μM range. We suggest that **1** targets bacterial cell division, as molecular docking studies predicted that viriditoxin (**2**) and mycopyranone (**1**) bind to the protein FtsZ in the same pocket.

Compound **1**[23] was isolated as an optically active ($[\alpha]_D^{23} = -229$) yellow amorphous powder, and its molecular formula was established as $C_{40}H_{46}O_{12}$ via HRESIMS.[24] Analysis of the ^1H, ^{13}C and HSQC NMR data indicated the presence of a chelated hydroxy group (δ_H 13.79), one phenolic proton (δ_H 9.67), two aromatic protons (δ_H 7.20, 6.79), two oxymethines (δ_H 4.48, 4.73), one aliphatic methine (δ_H 1.42), three methylene (δ_H 1.98, 1.29/1.65, 1.22/1.44), one methoxy (δ_H 3.86) and two methyl groups (δ_H 0.91, 0.94), as well as nine fully substituted carbons, including three oxygenated and a carbonyl (lactone) moiety (Table 1 and Figures S3, S4, and S6).

These data accounted for a molecular formula of $C_{20}H_{23}O_6$, indicating that **1** was a symmetric dimer. In general, the ^1H and ^{13}C NMR data of **1** resembled those reported for viriditoxin (**2**),[25] pigmentosin,[26] talaroderxines A and B,[27] vioxanthin,[28] and cladiosporinone,[29] with minor differences attributed to the aliphatic chain at C-3/C-3'.

Analysis of the 2D NMR data, in particular COSY and HMBC experiments (Figures S5 and S7), allowed the identification of key fragments of the molecule (Figure 1).

For example, the COSY data permitted the assignment of the spin system shown in black (Figure 1), which was confirmed by the HMBC correlations observed between H_3-15 to C-13 and C-14, H_3-16 to C-12, C-13 and C-14, H_2-14 to C-16, C-15 and C-13, H-13 to C-12, H_2-12 to C-14, C-13 and C-11, and H_2-11 to C-13, among others. The 9,10-dihydroxy-7-methoxy-naphthopyranone fragment was confirmed via HMBC correlations between H-3 to C-4a, C-4 and C-1, H-4 to C-4a, H-5 to C-6, C-5a and C-4, H-6 to, C-5, C-7, C-8 and C-9a, 9-OH to C-9a, C-9 and C-8, 10-OH to C-10a, and C-10, and H_3-17 to C-7 (Figure 1). The connection between the 3-methylpentenyl moiety to the naphthopyranone fragment was established based on the HMBC correlations observed among H_2-11 and C-3, and H-3 to C-11 and C-12 (Figure 1). Finally, the 8, 8' linkage between the homodimers was established based on the HMBC mutual correlation amongst H-6/H-6' and C-8 and C-8'.

The axial chirality of the molecule was determined by ECD (Figure 2). Briefly, the spectrum of **1** in MeOH showed both positive and negative Cotton effects at 254 and 274 nm, respectively, similar to those of viriditoxin (**2**),[25] talaroderxine B,[27] and *M*-vioxanthin.[28] The negative Cotton effect at 274 nm was attributed to the transitions of the naphthalene chromophores, indicating that the 8,8' axis in **1** was twisted in a counter-clockwise manner, characteristic for *M* axial chirality.[25–27]

The absolute configuration at C-4/C-4' was determined as *R* based on the results of the modified Mosher´s ester method (Figure 3).[30] The absolute configuration at C-3/C-3' was also determined as *R* by analysis of the NOESY experiment and analysis of the $^3J_{H-3-H-4}$, value (0.8 Hz) (Figures 3 and S8). Unfortunately, the absolute configuration at C-13 was not determined due to the high flexibility of the chain. Thus, the structure of compound **1** was elucidated as depicted, and assigned the trivial name mycopyranone.

The activity of mycopyranone (**1**) was evaluated against *Staphylococcus aureus* (strain SA1199)[21] and a clinically relevant methicillin-resistant strain (MRSA USA300 LAC, AH1263).[22] Compound **1** displayed promising antibacterial activity against both strains. Due to structural similarity to **2**, compound **1** likely functions as an FtsZ inhibitor.[18] Since FtsZ is highly conserved across many Gram-positive organisms,[18] the ability of pathogens to develop resistance to 6,6'- or 8,8' binaphthopyranone derivatives (including both compounds **1** and **2**) may be limited. The minimum inhibitory concentration (MIC) of compound **1** was ≤ 8.7 μM against both strains, and IC_{50} values were in the lower μM range (2.0 μM and 2.7 μM against SA1199 and AH1263, respectively; Figure 4).

Berberine, which was previously shown to target FtsZ in *Escherichia coli*,[13] was used as a positive control. Berberine's antimicrobial activity (IC_{50} = 69.5 μM, MIC 223 μM; Supporting Information, Figure S10) was consistent with previous reports.[13, 31, 32] In addition, the cytotoxic potential of compound **1** was evaluated against a panel of cancer cell lines, as described recently.[33] It did not show potent activity (IC_{50} value > 50 μg/mL), suggesting that **1** lacks toxicity against mammalian cells.

Based upon these results, and data from previous reports, we hypothesized that compound **1** binds to protein FtsZ, similar to viriditoxin (**2**), thereby inhibiting bacterial cell division.[18] To gain additional information about the putative binding site of mycopyranone (**1**) and viriditoxin (**2**) in FtsZ, molecular docking studies were carried out. Briefly, the results indicated that **1** and **2** bind to FtsZ (−5.09. and −6.60 kcal/mol, respectively) in a hydrophobic pocket conformed by the amino acids Arg-134, Pro-135, Gln-144, Pro-165, Asp-167, Arg-168, Asp-171, Ser-223, Ser-247, Pro-248, Leu-250, Glu-251, Ser-253, Val-255, Phe-315 and Asp-317 (Figures 5 and S11).

The forces that govern the interactions are mainly hydrogen bonds and van der Waals interactions (Figure 5). This pocket differs from those reported previously for the synthetic compounds PC190723,[9] TXA709[34, 35] and TXA6101,[17] revealing a potential new druggable site in the FtsZ protein of *S. aureus*.

Supplementary Material

Refer to Web version on PubMed Central for supplementary material.

Acknowledgements

This research was supported in part by P01 CA125066 from the National Cancer Institute and T32 AT008938 (fellowship to LKC) from the National Center for Complementary and Integrative Health, both part of the National Institutes of Health, Bethesda, MD, USA. NMR studies were performed in part at the Joint School of Nanoscience and Nanoengineering (JSNN), a member of the Southeastern Nanotechnology Infrastructure Corridor (SENIC) and National Nanotechnology Coordinated Infrastructure (NNCI), which is supported by the National Science Foundation (Grant ECCS-1542174). We thank Dr. Joanna Burdette from the University of Illinois at Chicago for cytotoxicity testing.

References

1. Boucher HW; Talbot GH; Bradley JS; Edwards JE; Gilbert D; Rice LB; Scheld M; Spellberg B; Bartlett J Clin Infect Dis 2009, 48, 1. [PubMed: 19035777]
2. Liang S; He Y; Xia Y; Wang H; Wang L; Gao R; Zhang M Int J Infect Dis 2015, 30, 1. [PubMed: 25447735]
3. World Health Organization, http://www.who.int/mediacentre/factsheets/fs194/en/ 2016, Accesed September 2017.
4. Centers for Disease Control and Prevention: Antibiotic resistance threats in the United States, 2013, http://www.cdc.gov/drugresistance/pdf/ar-threats-2013-508.pdf 2013, Accessed 04 September 2017.
5. Boucher HW; Talbot GH; Benjamin DK Jr.; Bradley J; Guidos RJ; Jones RN; Murray BE; Bonomo RA; Gilbert D Clin Infect Dis 2013, 56, 1685. [PubMed: 23599308]
6. Cole ST Philos Trans R Soc Lond B Biol Sci 2014, 369.
7. Chellat MF; Raguž L; Riedl R Angew Chem, Int Ed 2016, 55, 6600.
8. World Health Organization, http://www.who.int/dg/speeches/2011/WHD_20110407/en/ 2011, Accesed September 2017.
9. Haydon DJ; Stokes NR; Ure R; Galbraith G; Bennett JM; Brown DR; Baker PJ; Barynin VV; Rice DW; Sedelnikova SE; Heal JR; Sheridan JM; Aiwale ST; Chauhan PK; Srivastava A; Taneja A; Collins I; Errington J; Czaplewski LG Science 2008, 321, 1673. [PubMed: 18801997]
10. Erickson HP; Anderson DE; Osawa M Microbiol Mol Biol Rev 2010, 74, 504. [PubMed: 21119015]
11. Margolin W Nat Rev Mol Cell Biol 2005, 6, 862. [PubMed: 16227976]
12. Jaiswal R; Beuria TK; Mohan R; Mahajan SK; Panda D Biochemistry 2007, 46, 4211. [PubMed: 17348691]

13. Domadia PN; Bhunia A; Sivaraman J; Swarup S; Dasgupta D Biochemistry 2008, 47, 3225. [PubMed: 18275156]
14. Urgaonkar S; La Pierre HS; Meir I; Lund H; RayChaudhuri D; Shaw JT Org Lett 2005, 7, 5609. [PubMed: 16321003]
15. Kanoh K; Adachi K; Matsuda S; Shizuri Y; Yasumoto K; Kusumi T; Okumura K; Kirikae T J Antibiot 2008, 61, 192. [PubMed: 18503198]
16. Vollmer W Appl Microbiol Biotechnol 2006, 73, 37. [PubMed: 17024474]
17. Fujita J; Maeda Y; Mizohata E; Inoue T; Kaul M; Parhi AK; LaVoie EJ; Pilch DS; Matsumura H ACS Chem Biol 2017, 12, 1947. [PubMed: 28621933]
18. Wang J; Galgoci A; Kodali S; Herath KB; Jayasuriya H; Dorso K; Vicente F; González A; Cully D; Bramhill D; Singh S J Biol Chem 2003, 278, 44424. [PubMed: 12952956]
19. Details about the strain isolation and identification are given in the Supporting Information, and the sequence data for MSX61662 were deposited in GenBank (accession nos. MH700254, MH700255).
20. Raja HA; Miller AN; Pearce CJ; Oberlies NH J Nat Prod 2017, 80, 756. [PubMed: 28199101]
21. Kaatz GW; Seo SM Antimicrob Agents Chemother 1995, 39, 2650. [PubMed: 8592996]
22. Junio HA; Todd DA; Ettefagh KA; Ehrmann BM; Kavanaugh JS; Horswill AR; Cech NB J Chromatogr B 2013, 930, 7.
23. Mycopyranone (**1**): yellow amorphous powder: ^{1}H and ^{13}C-NMR see Table 1, and Figures S3 and S4 (Supporting Information); HRESIMS, [M+H]+= 719.3052 (calcd. for C40H47O12, 719.3062) (Figure S9).
24. For details about the extraction and isolation of compound **1** see the Supporting Information file.
25. Suzuki K; Nozawa K; Nakajima S; Kawai K.-i. Chem Pharm Bull 1990, 38, 3180.
26. Elix JA; Wardlaw JH Aust J Chem 2004, 57, 681.
27. Suzuki K; Nozawa K; Nakajima S; Udagawa S.-i.; Kawai K.-i. Chem Pharm Bull 1992, 40, 1116. [PubMed: 1394627]
28. Bode SE; Drochner D; Müller M Angew Chem, Int Ed 2007, 46, 5916.
29. Liu Y; Kurtan T; Yun Wang C; Han Lin W; Orfali R; Muller WEG; Daletos G; Proksch P J Antibiot 2016, 69, 702. [PubMed: 26905758]
30. Hoye TR; Jeffrey CS; Shao F Nat. Protocols 2007, 2, 2451. [PubMed: 17947986]
31. Yu HH; Kim KJ; Cha JD; Kim HK; Lee YE; Choi NY; You YO J Med Food 2005, 8, 454. [PubMed: 16379555]
32. Kellogg JJ; Todd DA; Egan JM; Raja HA; Oberlies NH; Kvalheim OM; Cech NB J Nat Prod 2016, 79, 376. [PubMed: 26841051]
33. Rivera-Chávez J; Raja HA; Graf TN; Burdette JE; Pearce CJ; Oberlies NH J Nat Prod 2017, 80, 1883. [PubMed: 28594169]
34. Kaul M; Mark L; Parhi AK; LaVoie EJ; Pilch DS Antimicrob Agents Chemother 2016, 60, 4290. [PubMed: 27161635]
35. Kaul M; Mark L; Zhang Y; Parhi AK; Lyu YL; Pawlak J; Saravolatz S; Saravolatz LD; Weinstein MP; LaVoie EJ; Pilch DS Antimicrob Agents Chemother 2015, 59, 4845. [PubMed: 26033735]

HIGHLIGHTS

- A new 8,8'-binaphthopyranone (mycopyranone, **1**) was discovered and elucidated.
- Absolute configuration was elucidated via NOESY, Mosher's esters, and ECD data.
- Active in vitro vs a clinically-relevant methicillin-resistant *S. aureus* strain.
- Molecular docking studies suggests binding to the FtsZ (tubulin-like) protein.

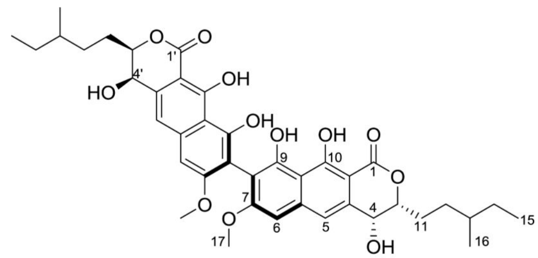

1

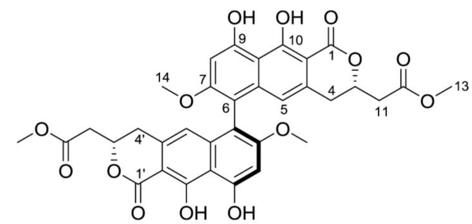

2

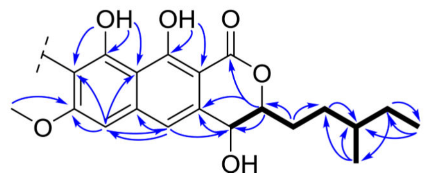

Figure 1.

Structures of mycopyranone (**1**) and viriditoxin (**2**) and key COSY (bold bonds) and HMBC correlations (arrows) for compound **1**.

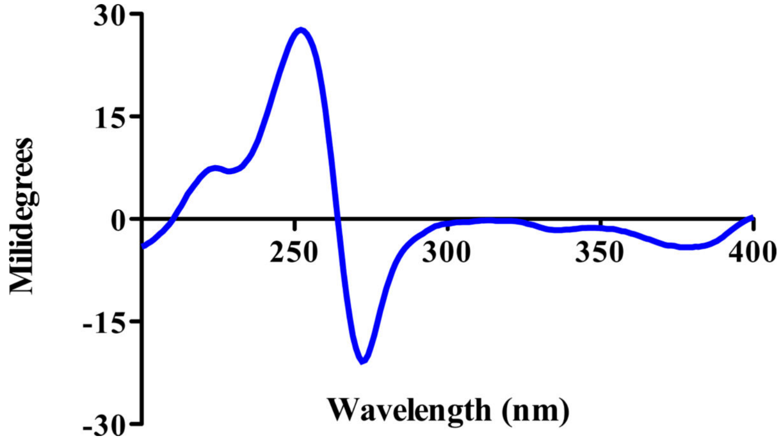

Figure 2.
ECD spectrum of **1** recorded in MeOH (13 μM)

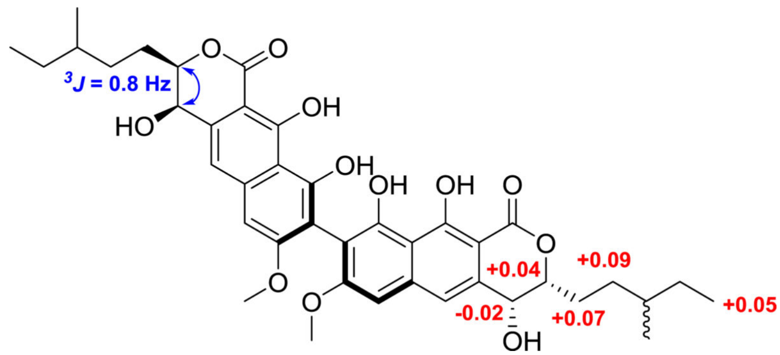

Figure 3.

$\Delta\delta_H$ values [$\Delta\delta$ (in ppm) = $\delta S - \delta R$] (red) from the Mosher's esters experiment and key NOESY correlation (blue arrow) and coupling constant, all observed for compound **1**.

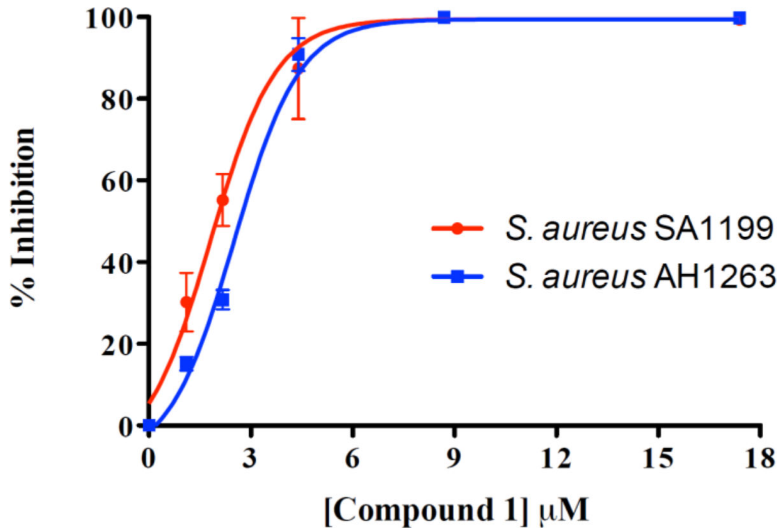

Figure 4.

Concentration-response curves of compound **1** against *S. aureus* SA1199 (red circles) and methicillin-resistant *S. aureus* AH1263 (blue squares). The minimum inhibitory concentration (MIC) of compound **1** was ≤ 8.7 μM against both *S. aureus* strains. The MIC of the positive control, berberine, was 223 μM against both *S. aureus* strains.

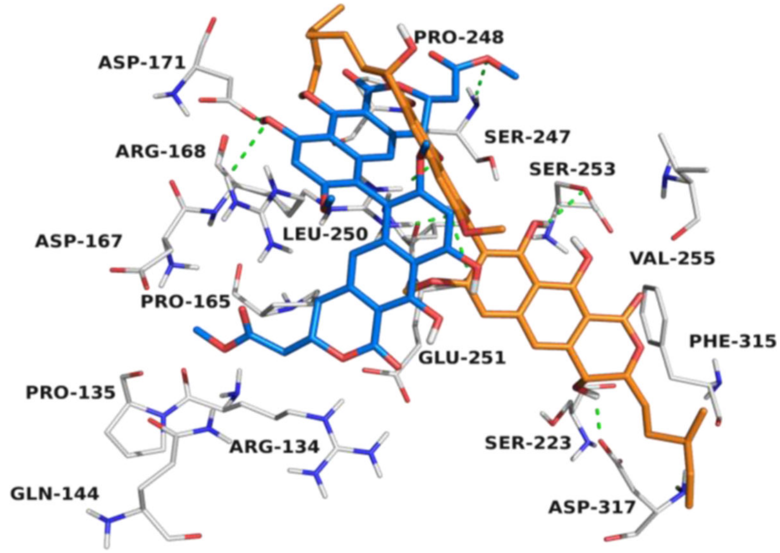

Figure 5.

Structural model of the predicted binding pocket for viriditoxin (**2**) (blue) and mycopyranone **1** (orange) with FtsZ (PDB 4DXD).

Table 1.

^1H and ^{13}C NMR data for compound **1** recorded in $CDCl_3$ at 700 MHz

Position	δ_C	type	δ_H, multiplicity (*J* = Hz)
1	171.0	C	
3	83.1	CH	4.48, *brt* (7.0)
4	66.9	CH	4.73, *brs*
4a	135.0	C	
5	117.3	CH	7.20, *s*
5a	140.1	C	
6	99.1	CH	6.79, *s*
7	161.7	C	
8	109.4	C	
9	155.6	C	
9a	109.2	C	
10	163.1	C	
10a	97.8	C	
11	28.0	CH_2	1.98, *m*
12a	32.0	CH_2	1.29, *m*
12b			1.65, *m*
13	34.5	CH	1.42, *m*
14	29.5	CH_2	1.22, *m*
			1.44, *m*
15	11.5	CH_3	0.91, *t* (7.3)
16	19.2	CH_3	0.94, *d* (6.5)
17	56.2	CH_3	3.86, *s*
4-OH			1.86, *brs*
9-OH			9.67, *s*
10-OH			13.79, *s*